



VISUALIZATION OF THE FLOW STRUCTURE BEHIND THE SHOCK FRONT USING TALBOT INTERFEROMETRY TECHNIQUE

M.V. DOROSHKO^a, P.P. KHRAMTSOV, O.G. PENYAZKOV

Luikov Heat and Mass Transfer Institute, Minsk, 220072, Belarus

^aCorresponding author: Tel.: +375172840668; Fax: +375172840668; E-mail: dormike@mail.ru

KEYWORDS:

Main subjects: gas dynamics, flow visualization, optical diagnostics

Fluid: incident shock wave, flow structure, boundary layer

Visualization method(s): Talbot interferometry

Other keywords: two-dimensional processing, image processing

ABSTRACT: The effect of self-reproduction, or Talbot effect is the basis of the proposed method of diagnostics. In this case the local deflection angles are determined at any point of the phase object with high spatial resolution, which is determined by the period of the Talbot grating. The advantages of this method are simplicity of implementation, the possibility of studying the entire flow field and the automatic processing of Talbot images. The above technique was used to study the flow structure behind the incident shock front.

The square shock tube with a cross section 50×50 mm was used to generate shock waves in the air with $M = 1.3-1.6$. Grids with square cells (12×12 and 3.5×3.5 mm) were used to initiate turbulence in the flow behind the shock wave.

Distributions of time-averaged density of the air throughout the whole flow field were calculated for the 12×12 and 3.5×3.5 mm grids. It is found that the thickness of the boundary layer in the observation area is about 7–9 mm, and the density in the boundary layer behind the shock front raises sharply. This leads to an increase of 6–7% of the average density of the flow at ≈ 3 mm from the shock tube wall.

INTRODUCTION. The understanding of the processes of mixing and transport in turbulent flows is a topical and relevant task both for research and for technical applications. On the other hand, the development of optical diagnostics of turbulent flows is a separate independent branch of fluid dynamics and provides deeper understanding of the physics of turbulent phenomena.

In the work [1] the visualization of the flow with variable density is carried out using conventional optical techniques such as shadow photograph and schlieren-method. It should be noted that the information obtained by such methods is likely to be of a qualitative nature. Speckle photography technique [2] provides quantitative information about the deflection angles of the whole investigated flow field. Based on the results of measuring deflection angles by the speckle photography method, the authors of the works [3, 4] showed how to change the visible structures of a turbulent flow after the passage of an incident shock wave.

With all the advantages of the speckle photography method as a quantitative method of optical flow diagnostics, we can't but mark the difficulties that arise during the processing of speckle images due to the effects of random interference and lack of sensitivity range of this method.

The technique of optical diagnostics of turbulent flows based on the Talbot effect [5] is completely free of the mentioned shortcomings. At the same time the deflection angles can be defined at any point of the phase object with high spatial density, which is determined by the period of a Talbot grating. Registration of ordered interference picture in the plane of self-reproduction provides several advantages in comparison with methods based on the effects of random interference due to a much greater sensitivity, spatial resolution and contrast of the resulting image. These features allow one to automate processing of Talbot image using computers and improve the measurement accuracy. In the works [6, 7] the Talbot effect was used to determine the distribution of helium average concentrations in the case of axisymmetric and two-dimensional jets outflows freely into the ambient air.

This research aimed to characterize the turbulent flow behind the incident shock wave with the help of the mentioned above technique.

EXPERIMENTAL SETUP AND THEORY. In Fig. 1 the developed for this research experimental setup scheme is shown. The square shock tube with cross-section 50x50 mm is used to generate shock waves of varying intensity. Interaction of the incident shock wave with the turbulizing grid creates velocity and density pulsations after the shock wave passage. Flow pulsations cause fluctuations of the local refraction index, which can be measured by Talbot - interferometer.

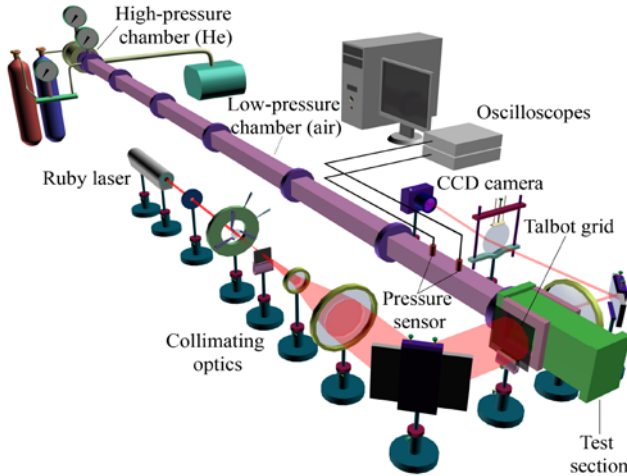


Figure 1. Experimental setup and optical scheme

duplicates the distribution on the grid [5]. The image on the screen is recorded with the required spatial and temporal resolution with the help of a digital camera.

Density of the neutral filter and the entrance aperture of the digital camera is chosen in such a way to obtain the optimum amount of light on the CCD recording matrix with exposures sufficient for averaging the turbulent fluctuations.

EXPERIMENTS. Turbulizing grids cause fluctuations of density and velocity following the incident shock wave in the test section of the shock tube. To initiate the turbulence in the flow behind the shock front the grids with 12x12 and 3.5x3.5 mm square cells were used.

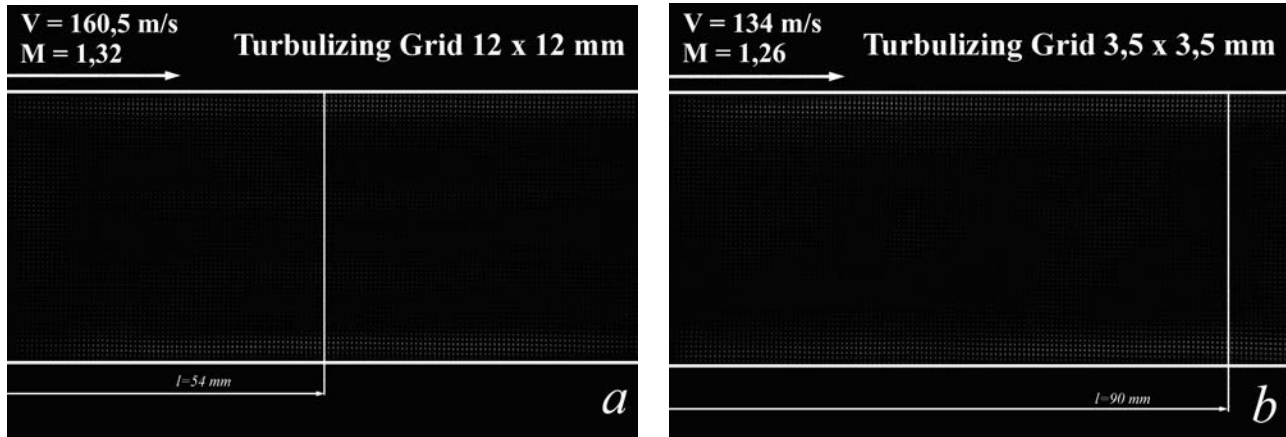


Figure 2. Difference images. Cell size: a) 12x12 mm; b) 3.5x3.5 mm

To avoid the influence of chemical reactions on turbulence characteristics, the experiments were carried out in the air. Mach number of the incident shock waves varied in the range $M = 1.3-1.6$. Fig. 2a and 2b show the difference images obtained by subtracting the intensities of illumination in the Talbot self-reproduction plane before and after the shock wave passage with 12x12 and 3.5x3.5 mm grids respectively. Illumination time is 400 microseconds. As seen from the difference images of time-averaged Talbograms, along with the local shift of the intensity maxima caused by the average deflection angles in the flow, these peaks are significantly blurred due to the turbulent fluctuations. The largest magnitude of shifting and blurring are observed near the tube wall in the boundary layer behind the shock wave. Every single element has approximately elliptical shape with different ratio of major and minor axes. This proves heterogeneity and nonisotropic characteristics of the fluctuations field. The mean calculated speed of the flow behind the shock wave in these experiments was 160.5 and 134 m/s.

VISUALIZATION OF THE FLOW STRUCTURE BEHIND THE SHOCK FRONT USING TALBOT INTERFEROMETRY TECHNIQUE

Fig. 3 illustrates the distribution of local deflection angles in the flow behind the shock wave for the tube cross-section (Fig. 2a and 2b). As can be seen from the figure, the greatest deflection angles and, consequently the highest density gradients in the flow are observed near the walls of the shock tube in the boundary layer. Thus, the greatest change in the density and deflection angles occurs across the flow.

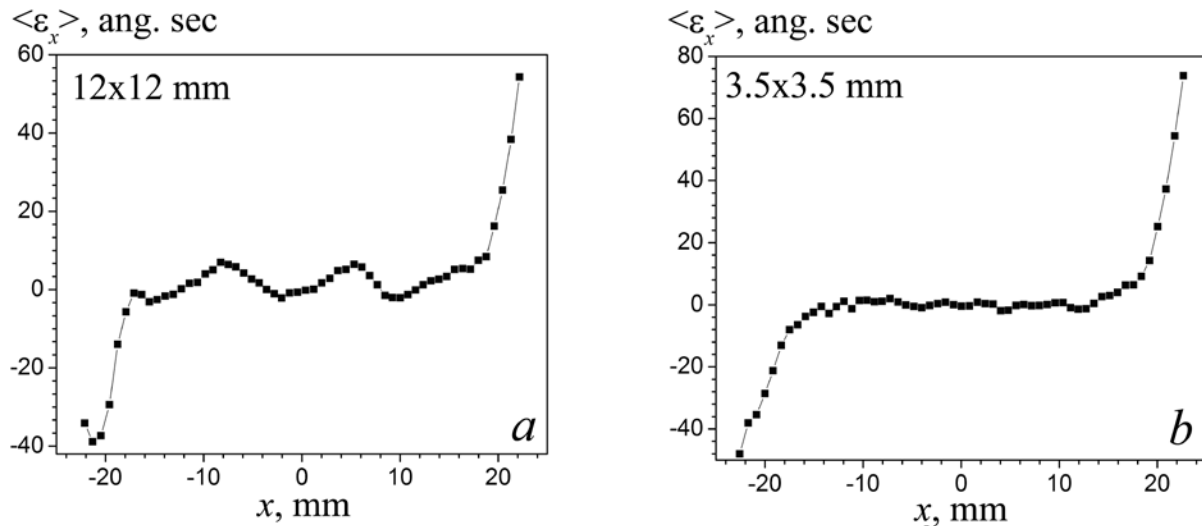


Figure 3. Distribution of local deflection angles in the flow behind the incident shock wave accordingly Fig. 2

The dependence of deflection angles for the 12×12 mm grid (Fig. 3a) in the middle has oscillations with a period $\approx 12\text{--}14$ mm, and for the 3.5×3.5 mm grid (Fig. 3b) is almost flat.

The data for the deflection angles can be numerically integrated, if the value of the refractive index of undisturbed medium is known [8]. Taking into account the fact that the mean density behind the shock wave can be calculated from initial conditions and the shock wave Mach, the absolute values of refraction indices and density of turbulent flow behind the shock wave can be found from the geometrical optics relations. The relationship between the refractive index and flow density is carried by the equation $n - 1 = K\rho$, where $K = 0,00022635 \text{ m}^3/\text{kg}$ – Gladstone-Dale constant [8].

RESULTS. In Fig. 4 the calculated distributions of the time averaged flow density in certain cross-sections of the shock tube is shown, based on the initial data in Fig. 3. In Fig. 5a and 5b is represented two-dimensional distribution of the air average density in the flow behind the shock wave for the 12×12 and 3.5×3.5 mm grids respectively.

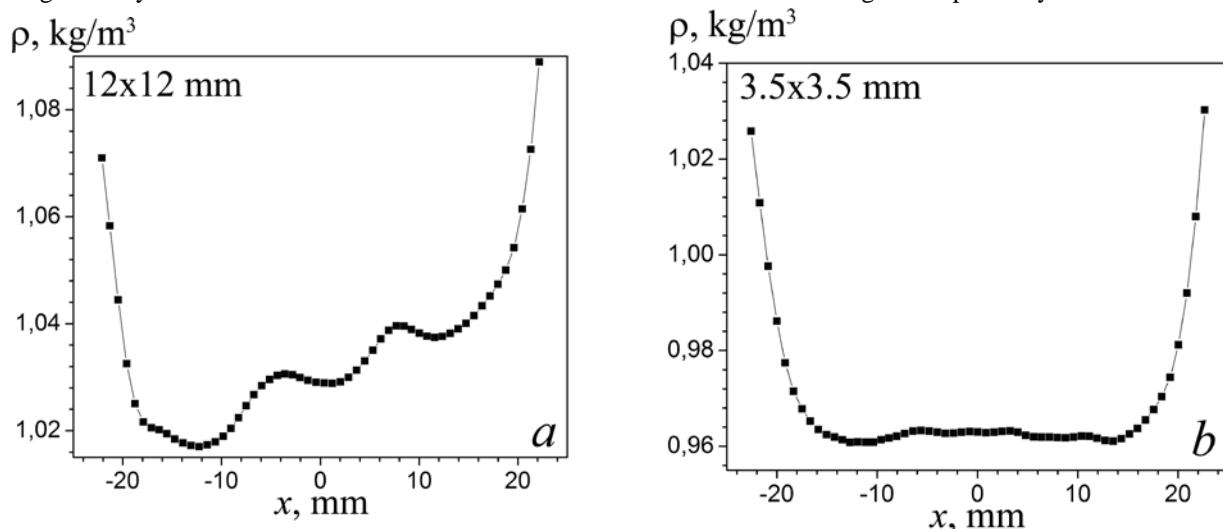


Figure 4. The distribution of the averaged air density in the flow behind the incident shock wave accordingly Fig. 2

As can be seen from the figures 4 and 5, the boundary layer thickness in the observation area is about 7–9 mm, and the density of the air in the boundary layer behind the shock front begins to increase sharply. This leads to the increase of

6–7% of the average flow density at the distance of ≈ 3 mm from the shock wall. Measurements show that for the case of the turbulizing grid with a cell of 12×12 mm (Fig. 4a and 5a), oscillation of the average flow density across tube have the scale ≈ 11 – 13 mm, which is comparable to the size of the cell. For the grid with a cell size of 3.5×3.5 mm the dependence of the average deflection angles across the tube is smoother. The absence of significant fluctuations of density in the core of the flow behind the shock wave is noted (Fig. 4b and 5b). This phenomenon can be explained by the specific nature of turbulence, or due to insufficient spatial resolution of this method.

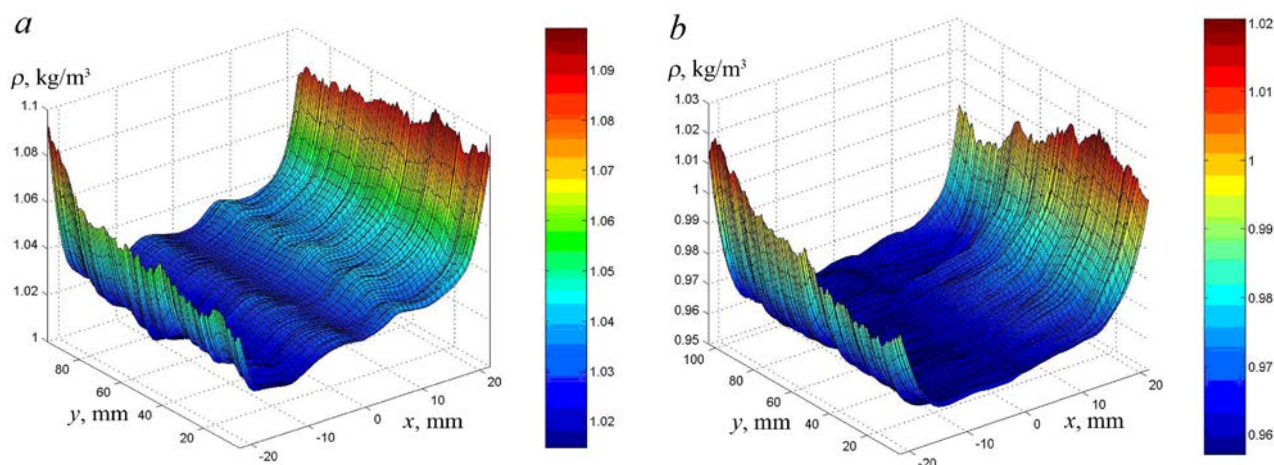


Figure 5. The distribution of the averaged air density in the flow behind the incident shock wave. Cell size: a) 12×12 mm; b) 3.5×3.5 mm

CONCLUSIONS. Applied possibilities of the Talbot-interferometry technique are illustrated by its usage for the density distribution measurements in the boundary layer behind the shock wave for different sizes of the turbulizing grids (12×12 and 3.5×3.5 mm).

Experiments show that the thickness of the boundary layer in a shock tube is 7–9 mm. Interaction in the wall boundary layer causes an increase of 6–7% of the average density of the flow at ≈ 3 mm from the shock tube wall.

This work was financially supported by Nanotech-1.26 and TA-56 programs.

References

1. Merzkirch W. Flow Visualization: second edition. Academic Press, Orlando. 1987.
2. Merzkirch W. // Experimental Thermal and Fluid Science. 1995. Vol. 10. Pp. 435–443.
3. Vitkin D., Merzkirch W., Fomin N. // Journal of Visualization. 1998. Vol.1, No.1. Pp. 29–35.
4. Fomin N., Lavinskaya E., Merzkirch W., Vitkin D. // Shock Waves. 2000. Vol. 10. Pp. 345–349.
5. Talbot, F. Facts relating to optical science. IV. // Philos. Mag. 1836. Vol. 9. Pp. 401–407.
6. Doroshko M.V., Penyazkov O.G., Rankin G., Sevruk K. L., Khramtsov P.P., Shikh, I.A. // J. Eng. Phys. Thermophys. 2006. Vol. 79. Pp. 937–942.
7. Doroshko M.V., Khramtsov P.P., Penyazkov O.G., Shikh I.A. // J. Eng. Phys. Thermophys. 2008. Vol. 81. Pp. 48–54.
8. Vasil'ev, L.A. Tenevye metody. Moscow: Nauka, 1968. 400 p [in Russian].